Antarct. Meteorite Res., **15**, 59–77, 2002

Estimation of three-dimensional internal structures of some barred olivine chondrules in Allende (CV3) chondrite

Takaaki Noguchi

Department of Materials and Biological Science, Ibaraki University, Bunkyo 2-1-1, Mito 310-8512 (tngc@mito.ipc.ibaraki.ac.jp)

Abstract: Three-dimensional internal structures of four BO chondrules in Allende were studied by stacking backscattered electron image photographs of their successive cross sections, which were taken by polishing very carefully these chondrules embedded in epoxy resin. The reconstructed structures show that the BO chondrules investigated are composed of several sets of parallel platy olivine crystals with smooth surfaces. The blanching of the crystals is relatively rare and the olivine plates occasionally have holes. The plates connect to the inner rims of the olivine shells. In a BO chondrule, altered mesostasis with unique texture was found in a restricted region of altered mesostasis, which contains "phlogopite". The "phlogopite"-bearing region is continuous to a sulfide nodule on the surface of the chondrule, which suggests that the volatile that formed "phlogopite" was introduced through a sulfide nodule on the surface of the chondrule.

1. Introduction

Petrologic studies of meteorites have been made on thin sections, in other words, two-dimensional information has been collected. Textures of various kinds of chondrules have been reproduced by many researchers since 1980s and are summarized by Hewins (1988). However, a kind of chondrules that are called barred olivine (BO) chondrules has not been well reproduced in laboratories in terrestrial environment. The formation conditions of BO texture have not been well constrained although there is general consensus that BO chondrules were heated at a temperature between complete and incomplete melting (*e.g.* Hewins, 1986; Radomsky and Hewins, 1990; Lofgren and Lanier, 1990; Lofgren *et al.*, 1996). They contain parallel skeletal olivine crystals, which are often crystallographically single (*e.g.* Wasson, 1974; Gooding and Keil, 1981; Weisberg, 1987), and further connected to the olivine shell, which is commonly observed in BO chondrules. Three-dimensional shape of the parallel skeletal olivine has not been investigated except for Tsuchiyama *et al.* (2000). To give constraints on the formation of BO chondrules, the most important information is the detailed morphology of the olivine "bars", three-dimensional arrangement of sets of the olivine "bars", and the relationship between the "bars" and the olivine shells. The author estimated three-dimensional internal structures of BO chondrules by polishing them very carefully. Although this is a destructive "low-tech" method, identification of mineral phases is easier and special resolution of each cross section is < 1 μm, which is much higher than non-destructive method such as high-resolution X-ray computed tomography (XCT) technique,

in which case, spatial resolution of two-dimensional sections is about 13 μm (Uesugi *et al.*, 1999).

The second purpose of the present work is to investigate spatial distribution of secondary minerals in chondrules to give insights on the alteration process. It is known that chondrules in CV3 chondrites experienced alteration (*e.g.* Krot *et al.*, 1995, 1998; Kimura and Ikeda, 1997). Ikeda and Kimura (1995) insisted that secondary Mg-Fe zoning of olivine, replacement of low-Ca clinopyroxene by Fe-rich olivine, replacement of primary mesostasis by nepheline and/or sodalite occurred in the solar nebula. However, Krot *et al.* (1995) selected an asteroidal origin of the secondary modification. Among all the CV chondrites, Allende is shown to have experienced the highest degree of such alteration (Kimura and Ikeda, 1997). Three-dimensional distribution of the secondary minerals would reflect the process of the alteration reaction.

2. Sample and method

Chips of Allende were gently crushed in an agate mill. After crushing, the chips were disaggregated into coarse-grained (most of them are composed of chondrules) and fine-grained fractions by the freeze-thaw method. Four barred olivine (BO) chondrules were selected under a stereomicroscope, based on the surface texture. In this paper, they were named as BO1 to BO4.

The chondrules were set in micromolds with flat bottom, which are usually used for TEM sample preparation, and then embedded in epoxy resin. BO1, BO2, and BO3 were embedded in the same micromold. BO4 were embedded in another micromold. The micromolds were removed after solidification of resin. The opposite side of the epoxy rod to the chondrules was cut and it was fixed by epoxy glue on the slide glass. The surface of the epoxy rods was polished. First, the surface was ground with #600 rotating grinder equipped on Maruto Preparap grinding machine. Parallelism between the sample mount and the rotating grinder is good enough, and it was pursued as careful as possible. About 10-μm material was removed in each step by using the indicator of the micrometer equipped on the machine. Next, the sample rods were carefully hand-lapped by using #2000 carborundum on an agate plate and polished with 1-μm diamond paste on a rotating polisher for a few minutes. After polishing, total thickness of the sample (sum of the thickness of the slide glass and the sample) was measured five times by a micrometer. Difference between the thickness of present time step and previous time step is the interval of one cross section. Variation of thickness of the sample rods was 2–4 μm. Figure 1 shows the variation of intervals between cross sections for two sample rods. As shown in Fig. 1a, intervals of each cross section in the sample rod including BO1 to BO3 are relatively even. The average for BO1 to BO3 was 46 μm $\pm$11 (1 σ). However, that for BO4 was fairly uneven as shown in Fig. 1b.

After carbon coating, backscattered electron images (BEIs) of each cross section were taken by JEOL JSM-5200 SEM at Ibaraki University. To use as guide to stack each BEI photomicrograph on proper position, optical photomicrographs of the each cross section were also taken under stereomicroscope. Each BEI photomicrograph was scanned by a flat bed scanner and processed by Adobe Photoshop 6.0 to make a mosaic BEI for each section, Scion Image to make projection stack for BO4, and Fortner Research T3D to

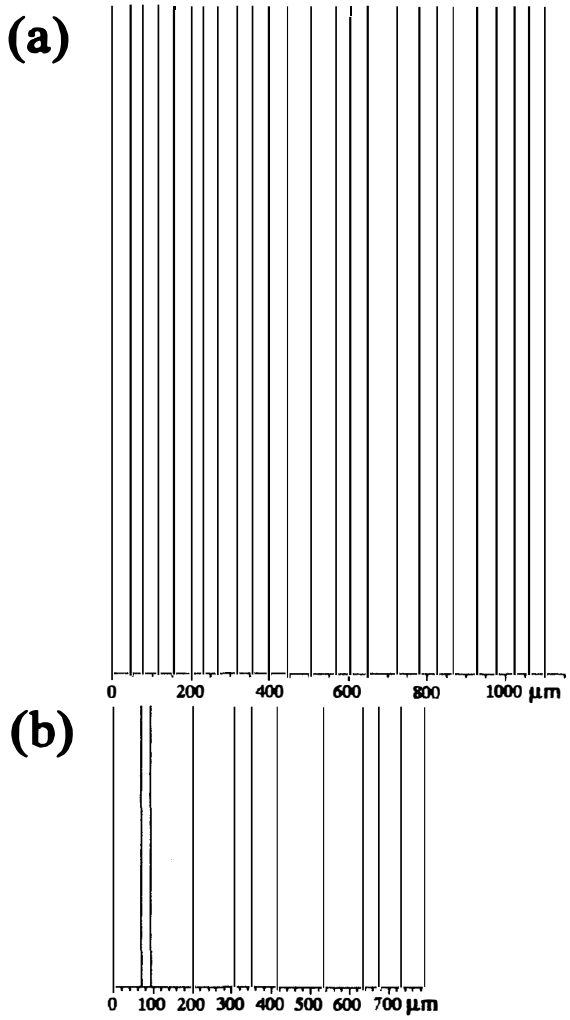

Fig. 1. Diagrams to show the intervals of cross sections for (a) BO1 to BO3 and (b) BO4. Length of lines in (a) and (b) indicates maximum diameter of BO2 and BO4, respectively.

make slice images of BO1 and BO2 from different directions. One to five BEIs were taken for each cross section. There is enough overlap between neighboring BEIs not to distort the images. Differences of brightness and contrast among BEIs in each mosaic photographs were adjusted by Adobe Photoshop 6.0. Brightness and contrast among each mosaic BEI were also adjusted by the software. However, it was difficult to make all the mosaic BEIs in a chondrule have uniform level of brightness and contrast. Because the precision of position determined by the optical micrographs was not good enough to stack images, position of each BEI was additionally adjusted on the display of PC.

In order to compare the present results with the other BO chondrules, petrography of thirty BO chondrules in three polished thin sections (PTSs) of Allende was investigated under an optical microscope. Cathodoluminescence (CL) images of a BO chondrule in the thin sections were taken by JEOL JSM-5900 equipped with Oxford CL2 at National Institute of Polar Research. In the case of BO4, electron microprobe analysis of minerals

in the cross sections no. 3 and no. 7 was performed. JEOL JXA-733 electron microprobe analyzer at Ibaraki University was used. Sample current was 9 nA and accelerating voltage 15 kV. A focused beam was used for the analysis of olivine, pyroxene, and plagioclase and 5 μm defocused beam for altered mesostasis. Bence and Albee analytical correction was applied. Detailed analytical conditions and detection limits were written in Noguchi (1995).

3. Results

3.1. Description of successive cross sections of each chondrule

Figure 2 shows that BEIs of typical cross sections of four BO chondrules investigated. BO1, BO2, and BO4 are typical BO chondrules with olivine shells. In these chondrules, interstices between olivine "bars" are filled by fine-grained minerals. Although chemical compositions of the interstitial minerals in BO1 and BO2 were not measured by electron microprobe, their similar texture to that in BO4 for which chemical composition of mesostasis was measured suggests that they are composed of secondary minerals formed during an alteration process. In these chondrules, pristine mesostasis seems not to be preserved. Microprobe analysis of BO4 chondrule suggests that the mesostases of these chondrules are composed of relict anorthitic plagioclase and augite and secondary minerals such as ferroan olivine, nepheline, and sodalite. BO4 chondrule contains most heavily altered mesostasis among the three chondrules, which contains altered mesostasis with phlogopite. Detailed description of the mesostasis of this chondrule will be shown later.

BO1 chondrule has a thick (about 400 μm in width) olivine shell, which contains thin Fe-rich veins (< 2–5 μm in width) and secondary Mg-Fe zoning along the veins and around tiny sulfide nodules. The olivine shell is composed of densely packed olivine crystals, although the outline of each crystal is vague. Olivine in the shell has compositional zoning around small particles (< 20 μm) of Fe-Ni metal and/or Fe sulfide (Fig. 2a). Some of them are indicated by arrows. A small amount of mesostasis was observed between olivine crystals. Olivine crystals that comprise the inner rim of the shell do not contain opaque particles. The thickness of opaque particle-free olivine rim is < 50 μm. As can be seen in Fig. 2a, some olivine "bars" connect to the olivine shell. On the other hand, elongated olivine crystals in the core of BO1 contain scarce Fe-rich veins and do not show remarkable secondary zoning. Apparent thickness of each olivine "bar" in BO1 is 20–40 μm. Most of the bars have smooth and straight edges along their long dimensions. Branching of olivine bars is rare.

BO2 also has a olivine shell with 200–300 μm thick (Fig. 2b), of which olivine is coarse grained. Elongated olivine crystals in the core of this chondrule often blanch to thinner "bars" (see the lower part of BO2 in Fig. 2b). Apparent thickness is 20–150 μm. The olivine "bars" include thin Fe-rich veins perpendicular to their long dimensions. Secondary Fe-enrichment was observed along the veins and fine-grained (< 20 μm) Fe-Ni metal and/or Fe sulfide particles, which are indicated by arrows in Fig. 2b.

BO3 chondrule has a thin (< 50 μm) olivine shell, which often cannot be delineated in the left-half of the chondrule (Fig. 2c). This chondrule contains abundant Ca-rich pyroxene along with a small amount of low-Ca pyroxene. Elongated olivine contains

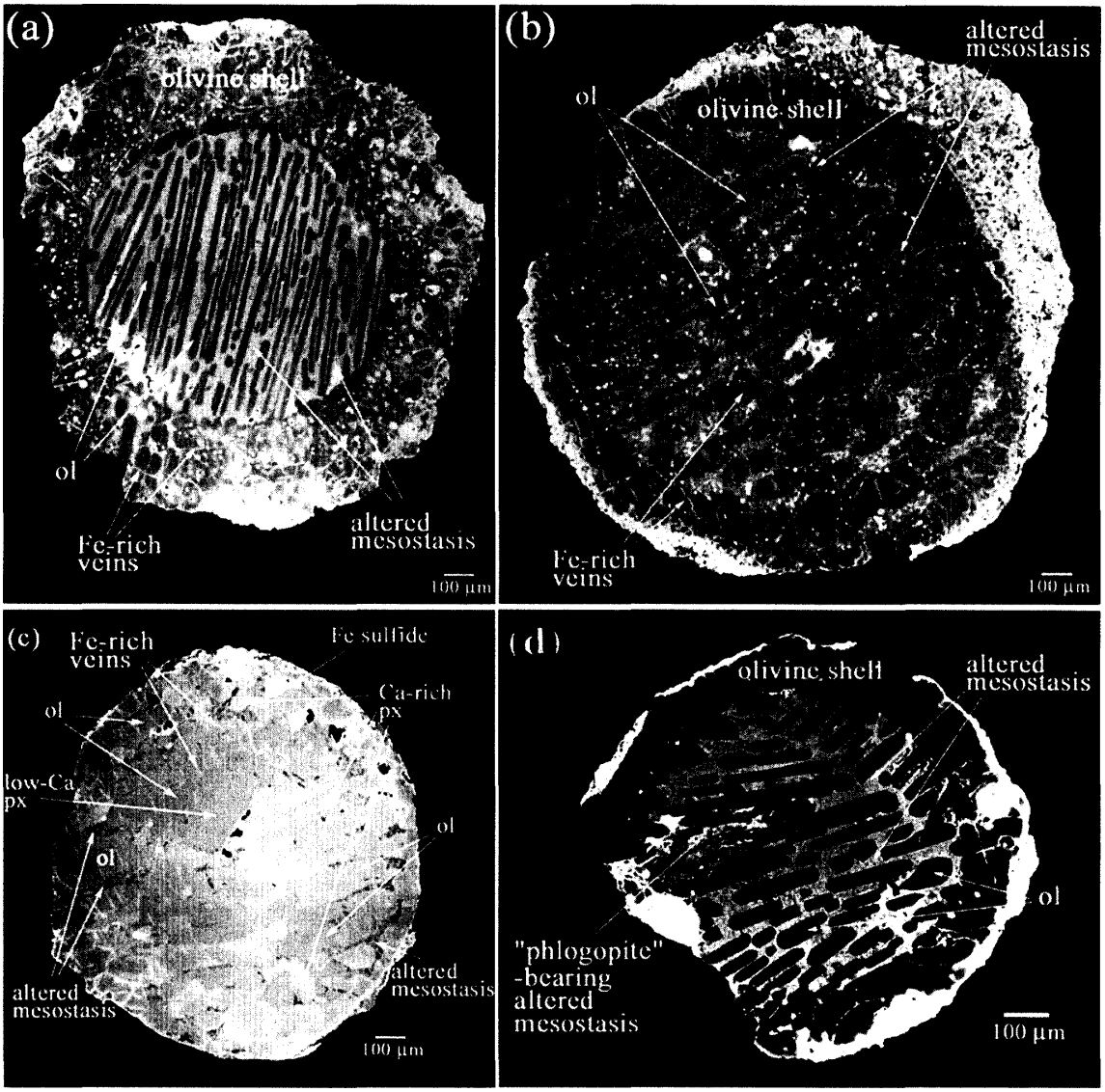

Fig. 2. BEI photomicrographs of typical cross sections of four BO chondrules investigated. (a) BO1. (b) BO2. (c) BO3. (d) BO4.

thin (< 5 μm) Fe-rich veins normal to its long axis, which are indicated by arrows in Fig. 2c. In this chondrule, olivine "bars" seem to be heterogeneous in chemical compositions. Olivine "bars" in the upper left part of the chondrule are more magnesian than those in right part. Apparent thickness of the olivine "bars" is 50–150 μm.

BO4 has a thick (about 100 μm in width) olivine shell (Fig. 2d). The grain size of olivine in the shell is coarse as well as BO2. Elongated olivine crystals in the core of BO4 have similar morphology and texture to that in BO1. Apparent thickness of the olivine "bar" is 20–50 μm. Iron-rich veins are rare in olivine in this chondrule although Fe-Mg compositional zoning was observed in olivine.

Figures 3 to 6 are successive cross sections of the four BO chondrules. In these successive photomicrographs, olivine crystals occur as "bars". In BO1, many olivine "bars" show one-to-one correspondence to the olivine "bars" in the next cross sections.

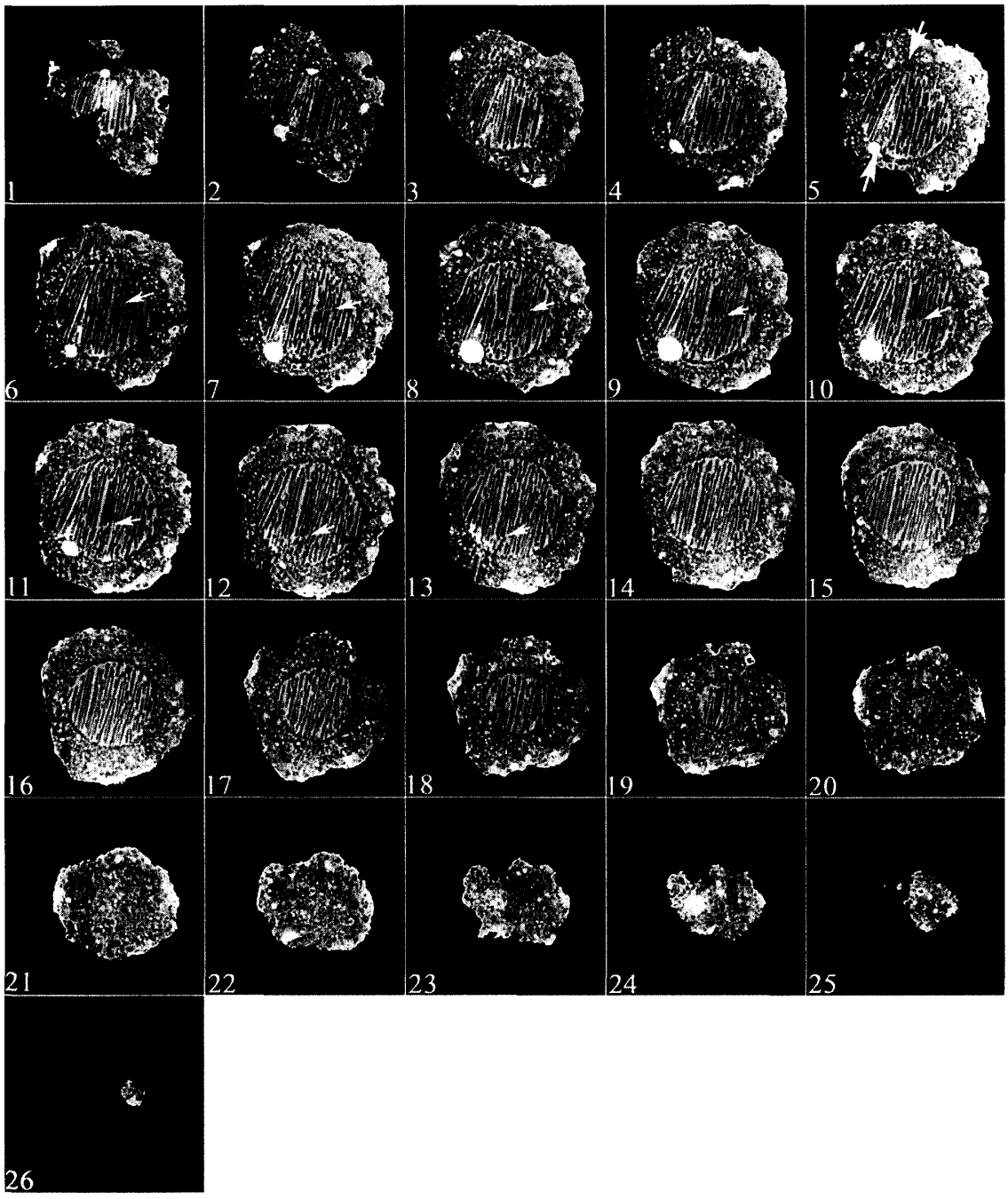

Fig. 3. Successive cross sections of the barred olivine chondrule No.1 (BO1). A pair of arrows in 3.5 is the boundary of two sets of olivine. Arrows in 3.6 to 3.13 indicate the same hiatus between olivine "bars".

This means that olivine "bars" are platy crystals that rarely have blanching. The thickness of olivine plates does not vary significantly. In BO1, two sets of olivine crystals that are composed of subparallel olivine "bars" can be easily recognized (Fig. 3). The boundary of the olivine sets is indicated by a pair of arrows in Fig. 3.5. It is note worthy that there are rare olivine crystals, conjunct to those in the other sets of olivine.

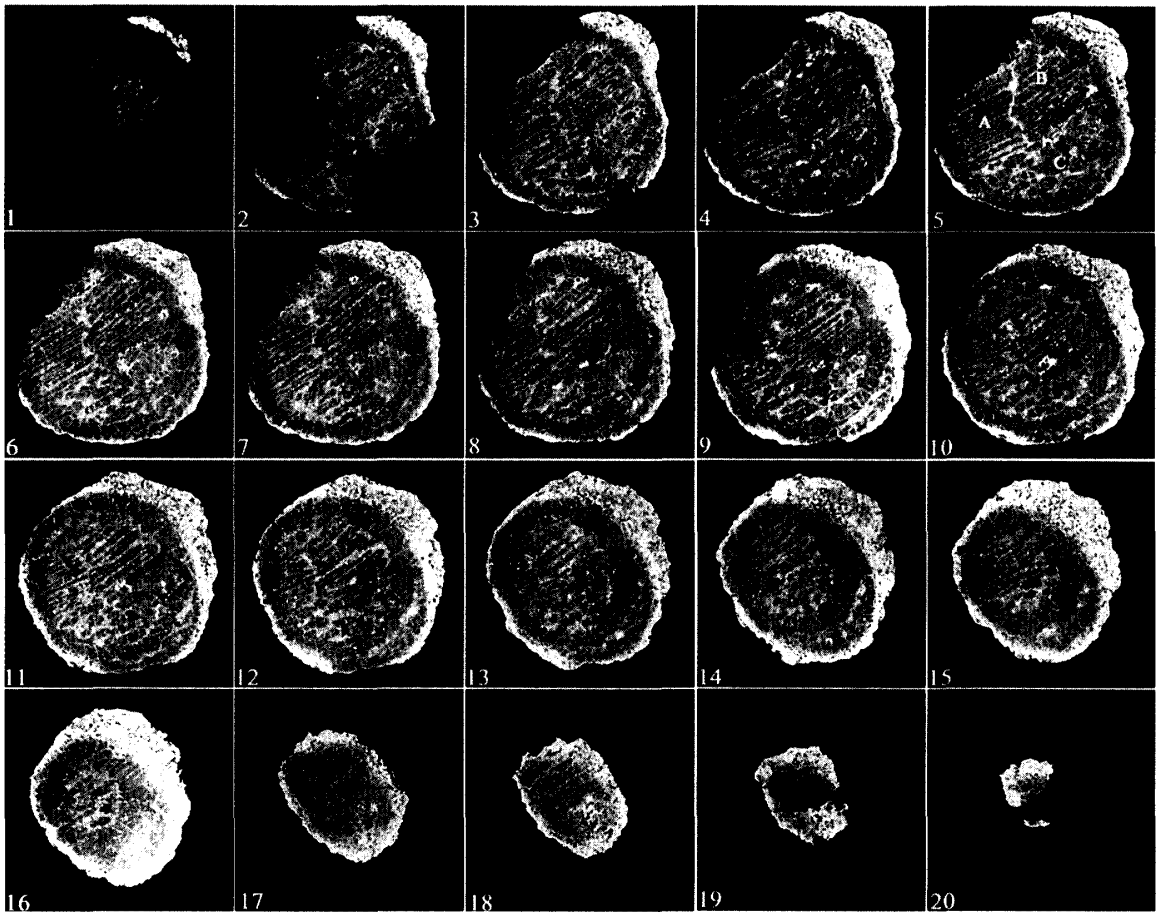

Fig. 4. Successive cross sections of the barred olivine chondrule No.1 (BO2). In 4.5, three sets of olivine labeled 'A' to 'C' are shown. Broken lines show the boundaries between them.

In the Figs. 3.6 to 3.13, there is a hiatus between olivine bars indicated by an arrow. The position of the hiatus systematically moves. The position of the hiatus may correspond to the boundary between olivine sets with slightly different orientations. The olivine plates that set above the arrows in Figs. 3.6 to 3.13 elongate almost through the chondrule. Olivine "bars" that attach to the olivine shell are relatively rare except for olivine "bars" in the left set in Fig. 3.5 and those in Figs. 3.19 and 3.20. Olivine plates belonging to a set attach the olivine shell locally. Based on the sequential images, discontinuous olivine "bars" are interpreted as platy crystals with pores that penetrate perpendicular to the tabular planes of olivine. Estimated dimension of this chondrule based on Fig. 3 is 1670 μm $\times$ 1470 μm $\times$ 1150 μm.

In BO2, three sets of olivine crystals are recognized (Fig. 4). The boundaries between three sets are indicated by broken lines in Fig. 4.5. Olivine crystals belonging to different sets rarely contact with each other as well as those in BO1. A olivine set composed of thin (20–40 μm in width) olivine "bars" labeled 'A' in Fig. 4.5 is shown in the middle left part of the chondrule. Most of the olivine crystals connect to the olivine shell. In the upper right portion of Fig. 4.5, second set composed of relatively thick olivine bars (40–150 μm in width) are seen (labeled 'B' in Fig. 4.5). Although many

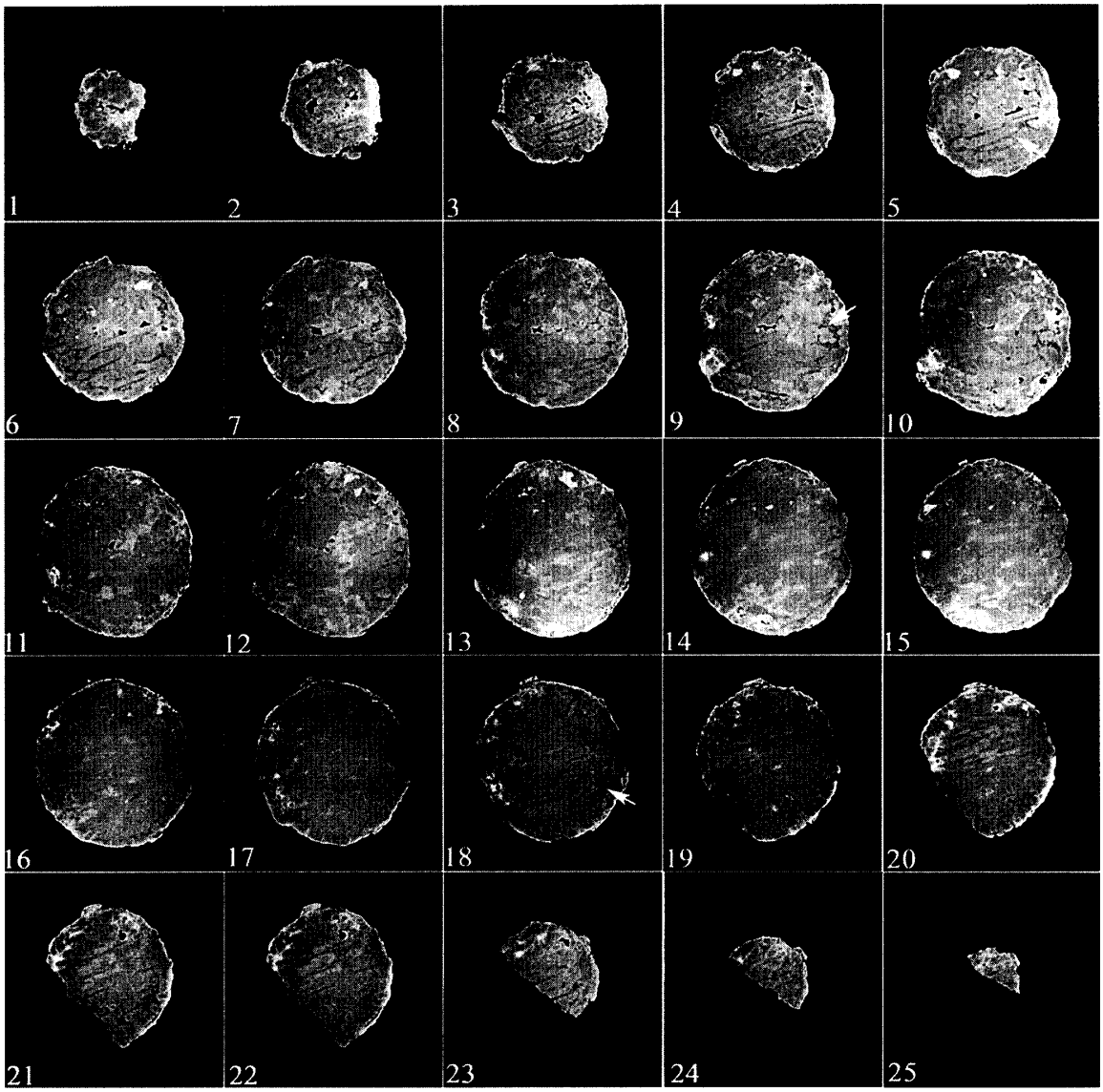

Fig. 5. Successive cross sections of the barred olivine chondrule No.1 (BO3). Arrows in 5.5, 5.9 and 5.18 indicate altered mesostasis.

olivine "bars" in this set also connect to the olivine shell, there are also hiatuses between the "bars" and the shell. Some instances of the hiatuses are indicated by arrows in Figs. 4.8 to 4.10. These figures also suggest that platy olivine crystals attach the olivine shell locally. Olivine crystals in the lower right labeled 'C' in Fig. 4.5 do not show "barred" texture. Looking from Fig. 4.3 to 4.16, one can recognize that the area of the olivine set 'A' in Fig. 4.5 decreases. On the other hand, the area of 'C' increases. Estimated dimension of this chondrule based on Fig. 4 is 1750 μm $\times$ 1685 μm $\times$ 870 μm.

BO3 is the most spherical among BO chondrules investigated. It has smooth surface, and the matrix is easily removed from the chondrule. In this chondrule, only one olivine set is distinguished (Fig. 5). The shape of olivine crystals is often difficult to delineate due to similar contrasts in BEIs between olivine and pyroxene that fill the

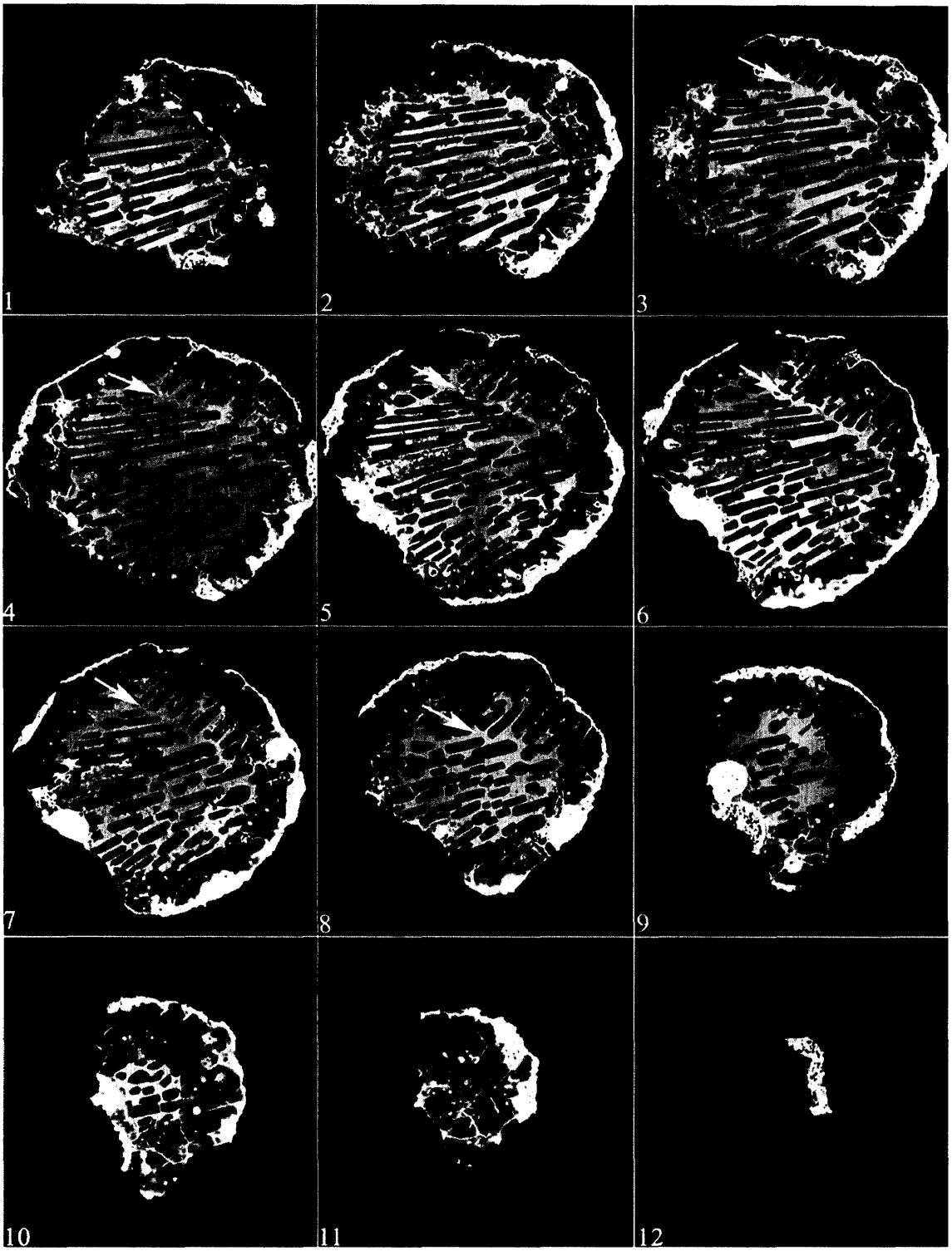

Fig. 6. Successive cross sections of the barred olivine chondrule No.1 (BO4). Arrows in 6.3 to 6.8 indicate the same hiatus between different sets of olivine.

interstices of olivine. Mesostasis was replaced by secondary minerals like the other chondrules investigated. Some of such altered mesostasis are indicated by arrows in

Figs. 5.6, 5.9, and 5.18. Estimated dimension of this chondrule based on Fig. 5 is 1370 μm $\times$ 1220 μm $\times$ 1100 μm.

BO4 contains olivine "bars" that have similar morphology to those in BO1. The olivine "bars" are platy crystals with minor blanches perpendicular to their wide planes (Fig. 6). At least three sets of olivine crystals with different orientations are recognized. In Figs. 6.1 and 6.2, only one set of subparallel olivine "bars" is present. From Fig. 6.3, another set that attaches to the upper right portion of the olivine shell appears. Like the other chondrules described above, these two sets of olivine rarely contact each other. The hiatuses are indicated by arrows in Figs. 6.3 to 6.8. Because a set of subparallel olivine appears in Fig.6.1 to 6.10, it clear that there are olivine plates elongated whole through the chondrule. Altered mesostasis in the middle left part of BO4 is partly lost as shown in Figs. 6.3 to 6.7. This area is more fragile than another area because this area experienced more severe alteration as shown in Fig. 2d. Estimated dimension of this chondrule based on Fig. 6 is 720 μm $\times$ 760 μm $\times$ 790 μm.

3.2. Reconstruction of three-dimensional internal structure of BO chondrules

Figures 7a–b is reconstructed three-dimensional internal structure of BO1 by stacking successive BEIs and show some examples of textural variation when the chondrule is cut in arbitrary directions. As shown in Figs. 7a and b, cross sections of the BO chondrule always contain olivine "bars" except for the case when the chondrules are cut almost parallel to the surfaces of planar olivine crystals. The probability that a BO chondrule is cut almost parallel to platy olivine crystals is thought to be low. Therefore, BO chondrules almost always display barred olivine texture.

3.3. Occurrence of "phlogopite"-bearing altered mesostasis in BO4

Electron microprobe analysis was performed for sections 3 and 7 of BO4. Olivine is magnesian while show compositional zoning. Olivines in sections 3 and 7 have similar chemical composition: olivine in the cores is Fo_{99} to Fo_{97} and Fo_{95} to Fo_{93} in the rims. A small amount of Ca-rich pyroxene was found. It is almost Fe-free and highly aluminous (18.4–18.9 wt%). A small amount of plagioclase ($An_{74}Ab_{25}Or_1$) was found.

Most of the mesostasis in BO4 is altered to secondary minerals such as ferroan olivine and nepheline with a considerable amount of Ca-bearing phases such as relict anorthitic plagioclase and Ca-rich pyroxene. Their chemical compositions are shown as altered mesostasis in Table 1. They are typically composed of < 5 μm across grains as shown in Fig. 8a, which is an enlarged BEI photomicrograph of section 7. There is also an area composed of an aggregate of thin (< 2 μm across) fibrous minerals. The altered mesostasis with this texture is developed in the sections 5 to 7. It contains less Al_2O_3 and CaO and more MgO and K_2O than altered mesostasis occupying most of the interstices of this chondrule. Figure 8c shows that the relationship between these oxide components in typical altered mesostases. The alerted mesostasis with unique texture is plotted between the normal altered mesostasis and phlogopite in Allende CAIs and chondrules (Hashimoto and Grossman, 1987; Kimura and Ikeda, 1996). This diagram and Table 1 suggest that the unique altered mesostasis possibly contains phlogopite. The altered mesostasis connects to a sulfide nodule that set at the surface of the chondrule (Figs. 6.5 to 6.7), suggesting that the mesostasis does not directly connect to the surface

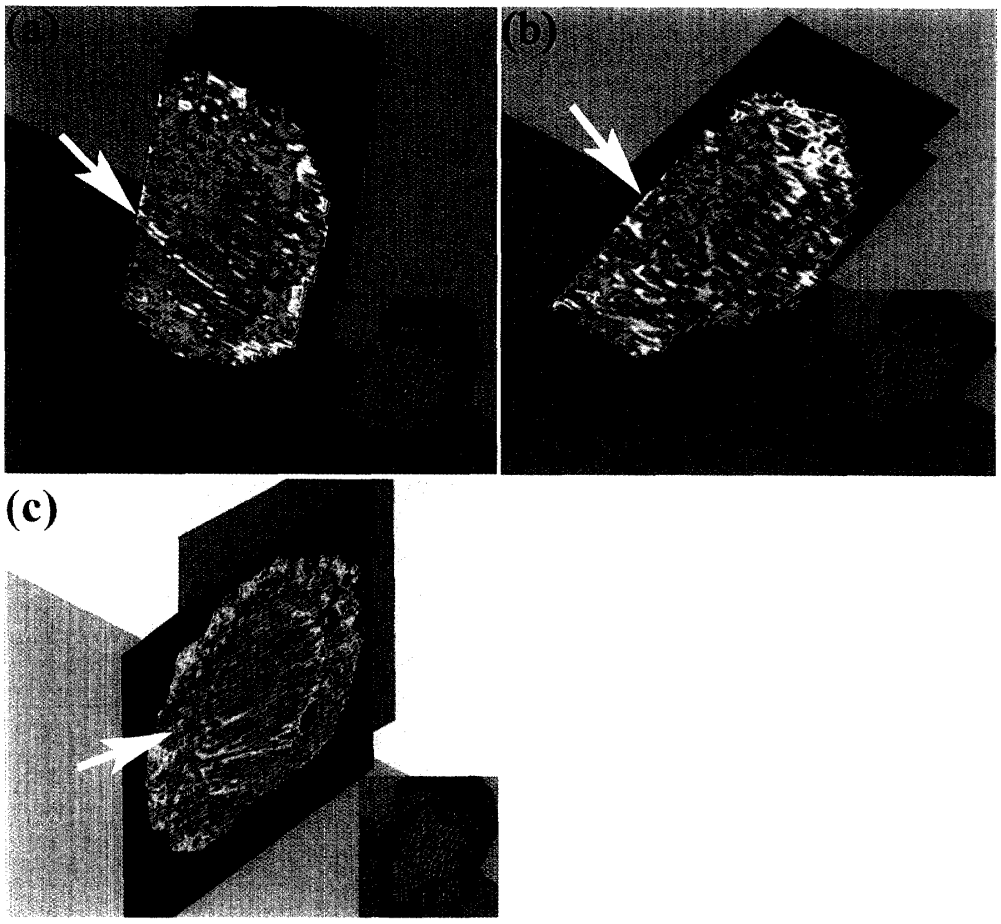

Fig. 7. Reconstructed cross sections of the BO1 chondrule. Light green area corresponds to olivine. Yellow and blue area interstitial to light green area corresponds to altered mesostasis. Yellow to red area on the periphery of BO1 corresponds to ferroan olivine. A red chunk at the inner boundary of BO1 in Fig. 7c is an opaque mineral-rich nodule. Insets show the cutting planes of the slices. Four cutting plates showing internal structures and four reconstructed chondrules with cutting planes are set near a wall of a virtual room. The boundary between a wall and a floor of a virtual room is indicated a straight line in each image. Virtual shadows (dark gray) of them are also shown in these images. The shapes and brightness of the shadows depend on the direction of light in the virtual rooms. Note that platy structures parallel to the stacking planes are artifacts due to the large intervals between the neighboring slices and due to different contrast and brightness among the mosaic BEIs of the slices. Directions of elongation of olivine "bars" are indicated by arrows.

of the chondrule, although microscopic path may be present.

4. Discussion

4.1. Three-dimensional structure of the BO chondrules in Allende and comparison with that in synthetic BO chondrules

Textural variation of BO chondrules in ordinary chondrites were investigated in detail by Weisberg (1987), and he displayed seven examples of BO chondrules in OCs. He found that "classic" BO chondrules that contains only one set of olivine crystals showing

Table 1. Some analyses of altered mesostasis in BO4.

sec. No.	3	3	7	7	phlogopite	phlogopite
occurrence	mesostasis	mesostasis	mesostasis*	mesostasis	in chondrule	in CAI
SiO_2	41.79	45.73	41.80	47.77	40.13	34.67
TiO_2	1.11	1.14	b. d.	0.71	0.66	n. d.
Al_2O_3	22.65	23.64	10.21	26.28	14.42	19.93
Cr_2O_3	n. d.	0.41	n. d.	0.13	0.29	n. d.
FeO	2.52	0.42	3.96	0.15	2.30	1.59
NiO	0.14	n. d.	n. d.	n. d.	2.38	n. d.
MnO	n. d.	n. d.	n. d.	n. d.	0.04	n. d.
MgO	11.03	4.68	31.33	4.15	20.81	22.79
CaO	8.34	19.82	5.06	18.33	4.31	1.52
Na_2O	4.13	1.35	1.60	1.97	1.55	3.46
K_2O	1.35	n. d.	1.42	n. d.	1.96	2.25
TOTAL	93.06	97.19	95.38	99.49	89.35	86.20
O=	22	22	22	22	22	22
Si	5.808	6.072	5.764	6.143	5.867	5.212
Ti	0.116	0.113	n. d.	0.069	0.072	n. d.
Al	3.710	3.699	1.659	3.983	2.484	3.543
Cr	n. d.	0.044	n. d.	0.013	0.033	n. d.
Fe	0.292	0.047	0.457	0.016	0.281	0.198
Ni	0.017	n. d.	n. d.	n. d.	0.281	n. d.
Mn	n. d.	n. d.	n. d.	n. d.	0.006	n. d.
Mg	2.285	0.927	6.440	0.795	4.536	5.097
Ca	1.243	2.822	0.748	2.525	0.673	0.248
Na	1.111	0.347	0.428	0.491	0.438	1.010
K	0.239	n. d.	0.250	n. d.	0.367	0.429
TOTAL	14.820	14.069	15.745	14.036	15.096	15.736

mesostasis*: altered mesostasis that seems to contain "phlogopite"
datum of phlogopite in chondrule: Kimura and Ikeda (1996)
datum of phlogopite in CAI: Hashimoto and Grossman (1987)
n. d.: not detected

simultaneous extinction under an optical microscope occupy about 10% of chondrules in ordinary chondrites (OCs). Most of the BO chondrites in OCs contain more than two sets of olivine. Based on the morphology of olivine crystals, they are divided into two groups. One includes elongated olivine crystals with smooth surfaces. In other words, blanching of the elongated olivine crystals is relatively rare. Another group contains olivine crystals with elongated dendritic or hopper morphology. He also found that pyroxene is often a major component in BO chondrules in OCs and that large (tens of μm) pyroxene grew at the expence of olivine. Crystallization of a similar BO chondrule with abundant pyroxene was discussed by Ikeda (1980).

All the BO chondrules investigated in this study belong to the former group. The BO chondrules except for BO3 have continuous olivine shells and contain more than two sets of olivine (Figs. 3, 4, 6). BO3 has the olivine shell that partially covers the surface

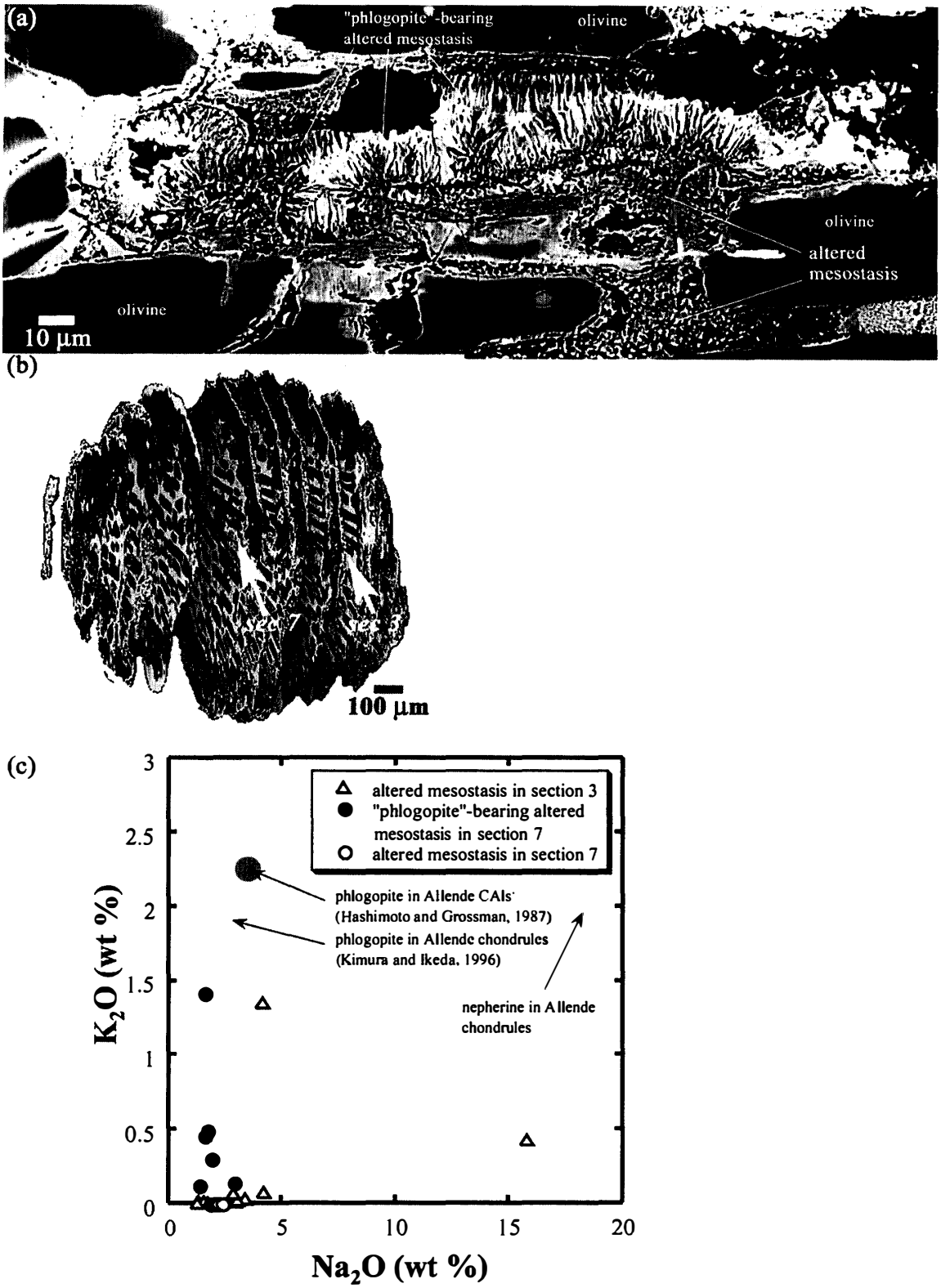

Fig. 8. Occurrence and chemical compositions of phlogopite-bearing altered mesostasis in BO4. (a) BEI of the phlogopite-bearing area in BO4. (b) A panel diagram of BO4. White arrows indicate sections 3 and 7. (c) Na_2O vs. K_2O wt% plot of altered mesostasis in sections 3 and 7 of BO4.

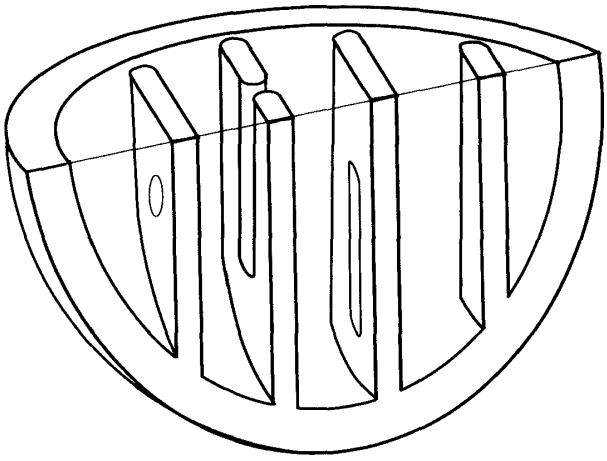

Fig. 9. A schematic figure of morphology of a set of olivine crystals in a one quarter piece of a BO chondrule. A set of olivine is composed of parallel platy olivine crystals with smooth surface. There are some holes in the olivine plates. The olivine crystals attach the inner surface of the olivine shell.

of the chondrule. In BO3, abundant low-Ca and Ca-rich pyroxenes fill the interstices of olivine without showing remarkable consumption of olivine. Therefore, central portion of the chondrule has almost holocrystalline texture (Fig. 5). Although these four BO chondrules are not "classic" BO as described above, they contain crystals with smooth surfaces like olivine in "classic" BO ones.

Common features of the platy olivine in the BO chondrules estimated from their sequential cross sections are summarized as follows: (1) the BO chondrules investigated are composed of more than two sets of subparallel platy olivine crystals, (2) the olivine plates are not dendritic or hopper crystals, (3) the BO chondrules have olivine shells, (4) the olivine plates are connected to the olivine shells, (5) the olivine plates attach a olivine shell locally, and (6) each set of olivine plates rarely contacts each other. A schematic model of a set of olivine plates is shown in Fig. 9. The shape of the individual olivine crystal is platy with some holes. The shape is similar to that of pyroxene crystals in radial pyroxene chondrules estimated by Fredriksson (1964). As shown in a set of olivine plates shown in the upper right portion of BO4 in Fig. 6.3 to 6.8, olivine plates seem to have crystallized from the olivine shell. The feature (6) may be due to almost simultaneous crystallization of different sets of olivine plates.

To evaluate whether these features are common to the other BO chondrules in Allende, thirty BO chondrules in three polished thin sections (PTS') of Allende were investigated under an optical microscope. BO chondrules including elongated hopper or dendritic olivine are relatively rare. Twenty-two among thirty contain platy olivine with smooth surfaces and olivine shells. Six contain elongated hollow olivine crystals, among which four do not have olivine shells. One with an olivine shell has thin platy to elongated hollow olivine with abundant pyroxene. Only one includes elongated dendritic olivine. The observation shows that most of the BO chondrules in Allende have olivine shells (25 among 30 BO chondrules). There are hiatuses between olivine plates and the olivine shells, which suggest that the plates attach the shell locally. It is thus concluded

that the features of the BO chondrules investigated are common to the BO chondrules investigated in the present study.

Formation conditions of BO chondrules have been estimated based on the dynamic crystallization experiments (*e.g.* Radomsky and Hewins, 1990b; Lofgren and Lanier, 1990). Dendritic barred textures were heated at around the liquidus temperatures although the absolute temperature varies depending on heating history (Connolly *et al.*, 1998). However, in these experiments, "barred" olivine crystals are dendritic and/or hopper, and the run products usually lack the olivine shells. Therefore, these experiments have not succeeded in reproducing the BO texture in a strict sense. Their textures rather resemble S type cosmic spherules with barred olivine textures (Brownlee, 1986). S-type spherules lack olivine shells. In the case of S-type spherules, ablation rather than evaporation may play a major role for mass loss during atmospheric entry heating.

Barred textures with olivine shells were recently reproduced by Tsukamoto *et al.* (1999, 2001) and Osada and Tsuchiyama (2001). In Tsukamoto *et al.* (1999, 2001), pulse heating experiments of olivine spheres were performed. The samples were heated to 2000°C for a few seconds by CO_2 laser then rapidly cooled by stopping the laser. They used aero-acoustic levitation to prevent contact with crucible wall. In their experiments, about 800°C supercooling was accomplished due to no contact with crucible wall. During cooling, the surface temperature again increased to a temperature near the melting point of olivine due to the recalescence phenomena. During the crystallization of olivine on the surface of the melt droplets, release of latent heat by crystallization represses additional nucleation of olivine. Therefore, olivine shells that composed of a small number of crystals were formed in their experiments. In Osada and Tsuchiyama (2001), FeO-rich starting material in a graphite capsule was melted by a gold image furnace. Because silicate melts do not wet graphite, the area where the melt contacted to a graphite capsule was very small. In this experiment, the pressure in the furnace was about 10^{-2} Pa at 1250 to 1430°C. During heating at about 1400°C for 10 min and subsequent cooling with a rate of 1000°C/hr, evaporation of FeO occurred from the surface of the samples. The surface of the samples became MgO-rich and the liquidus temperature became higher. Because larger supercooling was accomplished near the surface, crystallization started on the surface. The number of heterogeneous nucleation sites on the surfaces of the samples were probably kept low during crystallization due to minimum contact to the graphite capsule.

As shown above, different mechanisms were proposed to form olivine shells by these researchers. Tsukamoto *et al.* (1999, 2001) pointed out the importance of recalescence phenomena during crystallization of olivine on the surface of melt droplets. On the other hand, Osada and Tsuchiyama (2001) pointed out the importance of evaporation of FeO from the surface of melt droplets. In the case of Tsukamoto *et al.* (1999, 2001), starting materials are olivine. The run products were heated to above-liquidus temperatures. Natural chondrules are of multi-component systems, and therefore, it is not clear whether recalescence phenomena was important or not. Moreover, BO textures were formed even if the chondrules contain relict olivine. Figure 10 shows a "classic" BO chondrule including an unusually large euhedral olivine. Because the isolated olivine and the chondrule extinct almost simultaneously, a kind of topotaxial growth during crystallization of this chondrule is suggested (Figs. 10a, b). CL images of the large olivine grain clearly

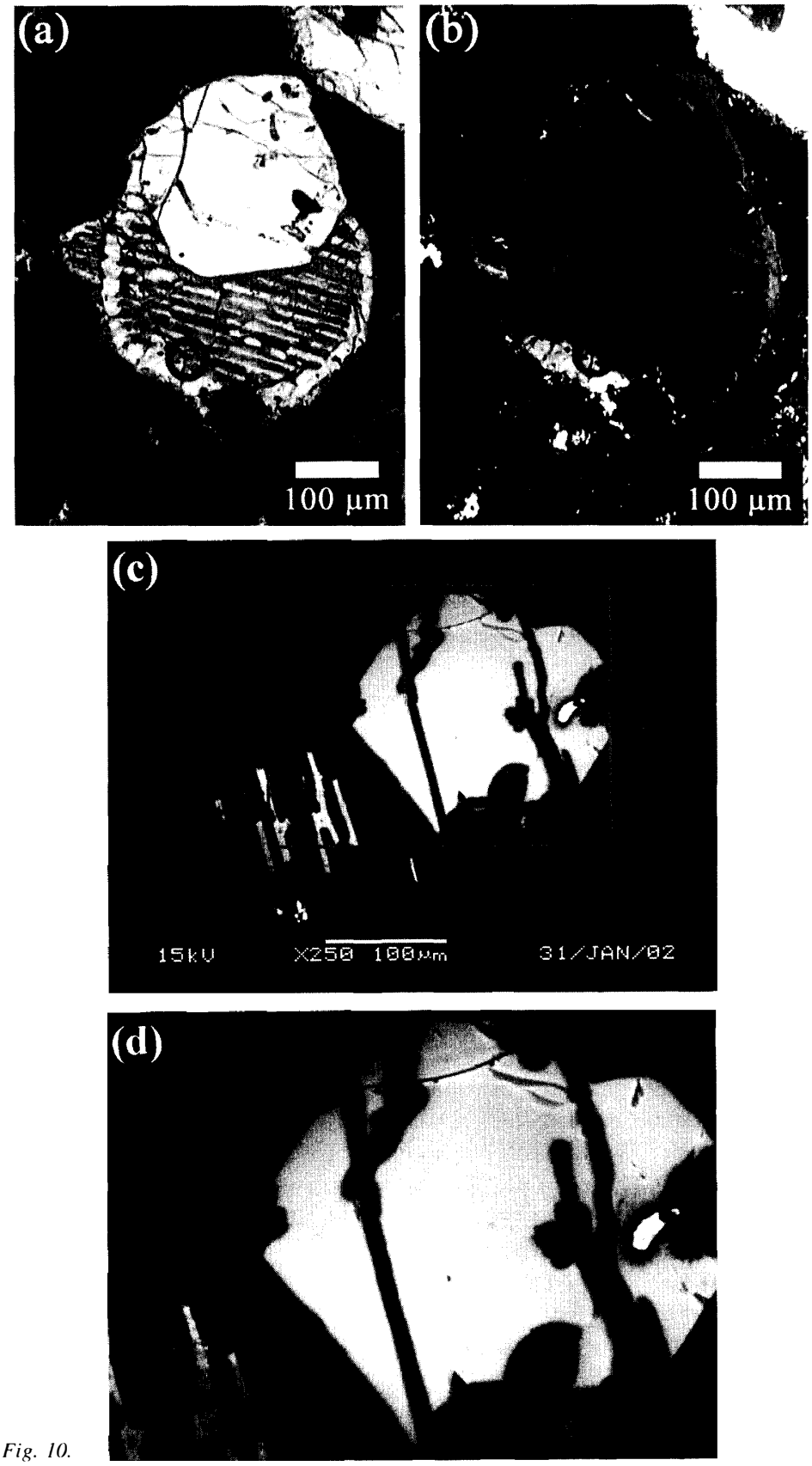

Fig. 10.

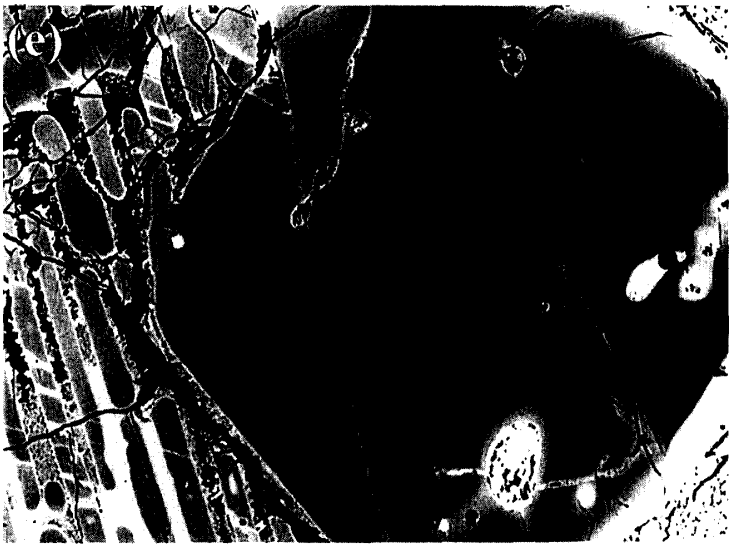

Fig. 10. Photomicrographs of a BO chondrule including a large euhedral olivine. On the surface of the chondrule, another small BO chondrule attaches. (a) open nicol. (b) cross nicol. These figures indicate that these components have almost the same crystallographic orientation. (c) CL image of this chondrule. A relict olivine having almost Fe-free compostion is shown as a large bright grain having a corroded form. (d) an enlarged CL image of the chondrules. The area of this image is indicated by a rectangular in (c). The relict olivine shows growth and sector zoning. (e) BEI of the same area in (d). Zoning cannot be seen in this image. The core of the relict grain contains a euhedral spinel grain.

show that it contains a relict with a corroded shape (Figs. 10c, d). Similar relict olivine was shown in Steele (1989, 1998) and Klerner *et al.* (2000). The relict olivine in the chondrule has growth and probably sector zoning, which cannot be observed in BEI photograph (Figs. 10d, e). These data of the BO chondrule clearly show that this BO chondrule was incompletely melted during chondrule formation. This observation is consistent with the general consensus that BO textures were heated at around the liquidus temperatures (*e.g.* Hewins, 1986; Radomsky and Hewins, 1990; Lofgren and Lanier, 1990; Lofgren *et al.*, 1996).

In the experiments by Osada and Tsuchiyama (2001), evaporation of FeO occurred because the experiments were performed in a vacuum furnace. They interpreted that olivine shells were formed though the evaporation of FeO from the surface of melt droplets. Such evaporation would have played an important role in the formation of BO chondrules because solar nebula pressure at 3 AU is thought to have been 1 to 10^{-2} Pa (Wood and Morfill, 1988). The parallel olivine crystals in the run products are, however, elongated dendritic or hopper, which differ from the natural ones. The other features of internal structure of BO chondrules investigated in this study have not been also reproduced yet.

One of the reasons why the morphology of the olivine crystals could not be reproduced in laboratories may be related to the difference of gravity between the real formation conditions and the terrestrial conditions. In the crystallization experiments under low gravity, growth forms of crystals are often quite different from those under 1 ***g***

(Tsukamoto *et al.*, 1999). Crystallization experiments from melt droplets with real BO compositions at low ambient pressure and low gravity may resolve an enigma of the formation conditions of the most common BO chondrules.

4.2. Spatial distribution of secondary minerals in BO chondrules in Allende

In BO4, "phlogopite"-bearing altered mesostasis occurs very locally. It is thought to be real crystalline phlogopite because a mica-group mineral has been identified from a BO chondrule in Allende by using synchrotron radiation X-ray diffraction technique (Noguchi *et al.*, 2001). The mesostasis experienced alteration to form secondary Mg-Fe zoning of olivine, replacement of low-Ca clinopyroxene by Fe-rich olivine, replacement of primary mesostasis by nepheline and/or sodalite (Ikeda and Kimura, 1995). Ikeda and Kimura (1995) and Kimura and Ikeda (1997) insisted that the alteration reactions occurred in the solar nebula although the possibility that these minerals were formed by metasomatic reactions in the meteorite parent body is not denied (Krot *et al.*, 1995, 1998). In BO4, the "phlogopite"-bearing area (Fig. 8) is restricted to a narrow area between two olivine plates and contacts to a sulfide nodule. The rare occurrence of the "phlogopite"-bearing area suggests that the reactant is not nebular gas. The connection of the sulfide nodule may suggest the introduction of volatiles through the nodule. Combined study of this method and high-resolution XCT like the case of Tsuchiyama *et al.* (2001) and identification of H_2O in phlogopite in chondrule are needed to check the nature of the reacted volatile and give a constraint for the formation condition of phlogopite.

Acknowledgments

Microprobe analysis and SEM observation of sequential cross sections of BO4 was performed by Mr. H. Honjyo (Ibaraki University). Dr. M. Kimura (Ibaraki University) gave the author data of phlogopite in Allende chondrules. The author thanks them. Dr. A. Tsuchiyama (Osaka University) is also appreciated for his advice to make cross cut images of chondrules by use of T3D. Drs. H. Nagahara (University of Tokyo) and A. Tsuchiyama are greatly appreciated for their constructive discussion and comments for the manuscript. CL images of a BO chondrule were taken at NIPR. The author thanks Dr. A. Yamaguchi for his instruction to take CL photomicrographs. This study was partly supported by the JSPS Grant-in-Aid for Scientific Research (#13440158).

References

Brownlee, D.E., Bates, B. and Beauchamp, R. H. (1986): Meteor ablation spherule as chondrule analogs. Chondrules and Their Origins, ed. by E.A. King. Houston, Lunar Planet. Inst., 10–25.

Connolly, H.C., Jr., Jones, B.D. and Hewins R.H. (1998): The flash melting of chondrules: An experimental investigation into the melting history and physical nature of chondrule precursors. Geochim. Cosmochim. Acta, **62**, 2725–2735.

Fredriksson, K. (1963): Chondrules and the meteorite parent bodies. Trans. N. Y. Acad. Sci. Ser. 2, **25**, 756–769.

Gooding, J.L. and Keil, K. (1981): Relative abundances of chondrule primary textural types in ordinary chondrites and their bearing on conditions of chondrule formation. Meteoritics, **16**, 17–43.

Hashimoto, A. and Grossman, L. (1987): Alteration of Al-rich inclusions inside amoeboid olivine aggregates in the Allende meteorite. Geochim. Cosmochim. Acta, **51**, 1685–1704.

Hewins, R.H. (1988): Experimental studies of chondrules. Chondrules and the Early Solar System, ed. by J.

F. Kerridge and M.S. Matthews. Tucson, Univ. of Arizona Press, 662–679.
Ikeda, Y. (1980): Petrology of Allan Hills-764 chondrite (LL 3). Mem. Natl Inst. Polar Res., Spec. Issue, **17**, 50–82.
Ikeda, Y. and Kimura, M. (1995): Anhydrous alteration of Allende chondrules in the solar nebula I: Description and alteration of chondrules with known oxygen-isotopic components. Proc. NIPR Symp. Antarct. Meteorites, **8**, 97–122.
Kimura, M. and Ikeda, Y. (1997): Comparative study of anhydrous alteration of chondrules in reduced and oxidized CV chondrites. Antarct. Meteorite Res., **10**, 191–202.
Klerner, S., Jones, R.H., Palme, H. and Shearer, C.K. (2000): Trace elements and cathodoluminescence in refractory forsterites from Allende and Kaba. Lunar and Planetary Science XXXI, Abstract #1689. Houston, Lunar Planet. Inst. (CD-ROM).
Krot, A.N., Scott, E.R.D. and Zolensky, M.E. (1995): Mineralogical and chemical modification of components in CV 3 chondrites: Nebular or asteroidal processing? Meteoritics, **30**, 748–775.
Krot, A.N., Petaev, M.I., Zolensky, M.E., Keil, K., Scott, E.R.D. and Nakamura, K. (1998): Secondary calcium-iron-rich minerals in the Bali-like and Allende-like oxidized CV3 chondrites and Allende dark inclusions. Meteorit. Planet. Sci., **33**, 623–645.
Lofgren, G.E. (1996): A dynamic crystallization model for chondrule melts. Chondrules and the Protoplanetary Disk, ed. by R.H. Hewins *et al.* Cambridge, Cambridge Univ. Press, 187–196.
Lofgren, G.E. and Lanier, A.B. (1990): Dynamic crystallization study of barred olivine chondrules. Geochim. Cosmochim. Acta, **54**, 3537–3551.
Noguchi, T. (1995): Petrology and mineralogy of the PCA 91082 chondrite and its comparison with the Yamato-793495 (CR) chondrite. Proc. NIPR Symp. Antarct. Meteorites, **8**, 33–62.
Noguchi, T., Kimura, M. and Osumi, K. (2001): Mica-group mineral in Allende CV3 chondrite investigated by synchrotron radiation X-ray diffraction method. Photon Factory Activity Report 2000, part B, **18**, 273.
Osada, Y. and Tsuchiyama, A. (2001): Experimental reproduction of rims in barred olivine chondrules by evaporation. Lunar and Planetary Science XXXII, Abstract #1334. Houston, Lunar Planet. Inst. (CD-ROM).
Radomsky, P.M. and Hewins, R.H. (1990): Formation conditions of pyroxene-olivine and magnesian olivine chondrules. Geochim. Cosmochim. Acta, **54**, 3475–3490.
Steele, I.M. (1989): Compositions of isolated forsterites in Ornans (C3O). Geochim. Cosmochim. Acta, **53**, 2069–2079.
Steele, I.M. (1998): Forsterite in ALHA 77307: Evidence for multiple origins. Lunar and Planetary Science XXIX, Abstract #1731. Houston, Lunar Planet. Inst. (CD-ROM).
Tsuchiyama, A., Uesugi, K. and Nakano, T. (2000): A study of three-dimensional structures of rocks and minerals using a high-resolution X-ray CT method—Primitive materials in the solar system and chondrules—. J. Geography, **109**, 845–858 (in Japanese).
Tsuchiyama, A., Uesugi, K., Noguchi, T., Yano, H., Nakano, T. and Suzuki, Y. (2001): Three-dimensional microstructures of Antarctic micrometeorites by X-ray computed microtomography using synchrotron radiation at Spring-8. Meteorit. Planet. Sci., **36**, Suppl., A210.
Tsukamoto, K., Satoh, H., Kobatake, H., Takamura, Y. and Kuribayashi, K. (1999): Towards the experimental space science in microgravity. Planetary People, **8**, 261–265 (in Japanese).
Tsukamoto, K., Kobatake, H., Nagashima, K., Satoh, H. and Yurimoto, H. (2001): Crystallization of cosmic materials in microgravity. Lunar and Planetary Science XXXII, Abstract #1846. Houston, Lunar Planet. Inst. (CD-ROM).
Uesugi, K., Tsuchiyama, A., Nakano, T., Suzuki, Y., Yagi, N., Umetani, K. and Kohmura, Y. (1999): Development of microtomography imaging system for rocks and mineral samples. Proc. SPIE, Developments in X-ray Tomography II, **3772**, 214–221.
Wasson, J.T. (1974): Meteorites. Berlin, Springer Verlag, 316 p.
Weisberg, M.K. (1987): Barred olivine chondrules in ordinary chondrites. Proc. Lunar Planet. Sci. Conf., 17th, pt. 2, E 663–E 676 (J. Geophys. Res., **92**, B4).
Wood, J.A. and Morfill, G.E. (1988): A review of solar nebula models. Chondrites and the Early Solar System, ed. by J.F. Kerridge and M.S. Matthews. Tucson, Univ. of Arizona Press, 329–347.

(Received December 12, 2001; Revised manuscript accepted January 29, 2002)